

Room evacuation through two contiguous exits

I.M. Sticco

*Departamento de Física, Facultad de Ciencias Exactas y Naturales, Universidad de Buenos Aires,
Pabellón I, Ciudad Universitaria, 1428 Buenos Aires, Argentina.*

G.A. Frank

*Universidad Tecnológica Nacional, Facultad Regional Buenos Aires,
Av. Medrano 951, 1179 Buenos Aires, Argentina.*

C.O. Dorso*

*Departamento de Física, Facultad de Ciencias Exactas y Naturales, Universidad de Buenos Aires, and
Instituto de Física de Buenos Aires, Pabellón I,
Ciudad Universitaria, 1428 Buenos Aires, Argentina.*

(Dated: March 8, 2022)

Current regulations demand that at least two exits should be available for a safe evacuation during a panic situation. Although the “faster is slower” effect is expected to take place near the exits, the evacuation time will improve because of the additional exits. However, rooms having contiguous doors not always reduce the leaving time as expected. We investigated the relation between the doors separation and the evacuation performance. We found that there exists a separation distance range that does not really improve the evacuation time, or it can even worsen the process performance. To our knowledge, no attention has been given to this issue in the literature. This work reports how the pedestrians dynamics differ when the separation distance between two exit doors changes and how this affects the overall performance.

PACS numbers: 45.70.Vn, 89.65.Lm

I. INTRODUCTION

The practice of providing two doors for emergency evacuation can be traced back to the last Qing dynasty in China (1644-1911 AD). A mandatory regulation established that large buildings had to provide two fire exits [1]. This kind of regulations upgraded to current standard codes with detailed specifications on the exits position, widths and separations [2, 3].

Current regulations claim that the minimum door width should be 0.813 m while the maximum door-leaf should not exceed 1.219 m [3, 4]. If more than two doors are required, the distance between two of them must be at least one-half or one-third of the room diagonal distance. But, no special requirements apply to the rest of the doors, regardless the fact that they should not be simultaneously blocked [3, 4].

The rulings leave some space for placing the extra openings (*i.e.* those above two exits) at an arbitrary separation distance. Thus, it is possible to place a couple of doors on the same side of the room. The special case of two contiguous doors has been examined throughout the literature [5–8].

Kirchner and Schadschneider studied the pedestrians evacuation process through two contiguous door using a cellular automaton model [5]. The agents were able

to leave the room under increasing panic situations for behavioural patterns varying from individualistic pedestrians to strongly coupled pedestrians moving like a *herd*. The evacuation time was found to be independent of the separation distance for the individualistic pedestrians in a panic situation. But if the pedestrians were allowed to move like a herd, an increasing evacuation time for small separation lengths (less than 10 individuals size) was reported.

The total number of pedestrians leaving the room per unit time actually showed a slow-down for separation distances smaller than four door widths [6]. This slow-down was identified as a disruptive interference effect due to pedestrians crossing in each other’s path. The threshold of four door widths ($4d_w$) corresponds to the distance separation necessary to distinguish two independent groups of pedestrians, each one surrounding the nearest door.

Researchers called the attention on the fact that no matter how separated the two contiguous doors are placed, the overall performance does not improve twice with respect to a single exit (of the same width). This effect is attributed to some sort of pedestrians interference [6].

Although the above results were obtained for very narrow doors (*i.e.* single individual width), further investigation showed that they also apply to doors allowing two simultaneous leaving pedestrians. However, this does not hold for a room with a single door [7]. In this case, it is true that the mean flux of evacuating people increases

* codorso@df.uba.ar

with an increasing door width, but the flux per unit width decreases [7].

The separation distance of the two doors may worsen the evacuation performance if the doors are placed close to the end of the wall, that is, near each corner of the room. People can get in contact with other walls, loosing evacuation efficiency [5, 7].

More detailed investigation on cellular automata evacuation processes showed that the evacuation performance depends on five distances: the total width of the openings (that is, adding the widths of each door), the doors separation distance, the width difference between the two doors, and the distance to the nearest corner [8].

The total width of the openings can improve the evacuation time for any separation distance between doors, if both doors have the same width. The door separation, however, controls the optimal location for these exits. A rough rule states that the doors separation distance d_g should equal $L - 4d_w$, where L is the room length [8].

The optimal location rule agrees with the slow-down phenomenon for small values of d_g . It also agrees with the worsening of the evacuation performance for doors close to a corner. But this kind of worsening may also appear for other reasons, since it has been suggested that the relatively longer traveling distance of the pedestrians to the doors also plays an important role.

The two doors configuration does not need to be symmetric along the wall. Asymmetry causes delays depending on the width difference between the doors and their relative position. It has been shown that placing the wider door in the middle of the wall, and another one at the corner (with reduced width), causes an improvement in the evacuation process [8].

Our investigation focuses only symmetric configurations with equal sized doors. As opposed to the above mentioned literature, we examine the evacuation dynamics by means of the Social Force Model (SFM). An overview of this model can be found in Section II.

In Sections II and III the single door configuration is revisited. Its purpose is to make easier the understanding of the two-doors configuration for very small separation distances d_g .

In Sections III and IV we examine the effects of increasing the d_g until the clogging areas close to each door become almost independent.

Section V resumes the pedestrians behavioural patterns, and its consequences on the evacuation performance, for the different door separation scenarios.

II. BACKGROUND

A. The Social Force Model

The “social force model” (SFM) deals with the pedestrians behavioural pattern in a crowded environment. The basic model states that the pedestrians motion is controlled by three kind of forces: the “desire force”, the “social force” and the “granular force”. The three are very different in nature, but enter into an equation of motion as follows

$$m_i \frac{d\mathbf{v}^{(i)}}{dt}(t) = \mathbf{f}_d^{(i)}(t) + \sum_j \mathbf{f}_s^{(ij)}(t) + \sum_j \mathbf{f}_g^{(ij)}(t) \quad (1)$$

where m_i is the mass of the pedestrian i , and \mathbf{v}_i is its corresponding velocity. The subscript j represents all other pedestrians (excluding i) and the walls. \mathbf{f}_d , \mathbf{f}_s and \mathbf{f}_g are the desire force, the social force and the granular force, respectively.

The desire force resembles the pedestrian’s own desire to go to a specific place [9]. He (she) needs to accelerate (decelerate) from his (her) current velocity, in order to achieve its own willings. As he (she) reaches the velocity that makes him (her) feel comfortable, no further acceleration (deceleration) is required. This velocity is the “desired velocity” of the pedestrian $\mathbf{v}_d(t)$. The expression for \mathbf{f}_d in Eq. (2) handles this issue.

$$\begin{cases} \mathbf{f}_d^{(i)}(t) &= m_i \frac{\mathbf{v}_d^{(i)}(t) - \mathbf{v}_i(t)}{\tau} \\ \mathbf{f}_s^{(ij)} &= A_i e^{(r_{ij}-d_{ij})/B_i} \mathbf{n}_{ij} \\ \mathbf{f}_g^{(ij)} &= \kappa(r_{ij} - d_{ij}) \Theta(r_{ij} - d_{ij}) \Delta \mathbf{v}_{ij} \cdot \mathbf{t}_{ij} \end{cases} \quad (2)$$

τ means a relaxation time. Further details on each parameter can be found in Refs. [9–13].

Notice that the desired velocity \mathbf{v}_d has magnitude v_d and points to the desired place in the direction $\hat{\mathbf{e}}_d$. Thus, v_d represents his (her) state of anxiety, while $\hat{\mathbf{e}}_d$ indicates the place where he (she) is willing to go. We assume, for simplicity, that v_d remains constant during an evacuation process, but $\hat{\mathbf{e}}_d$ changes according to the current position.

The social force \mathbf{f}_s corresponds to the tendency of each individual to keep some space between him and other pedestrian, or, between him and the walls [14]. The \mathbf{f}_s expressed in Eq. (2) depends on the inter-pedestrian distance d_{ij} . The magnitude $r_{ij} = r_i + r_j$ is the sum of the pedestrian’s radius, while A_i and B_i are two fixed parameters ($r_j = 0$ for the interaction with the wall). Thus, \mathbf{f}_s is a repulsive monotonic force that resembles

the pedestrian feelings for preserving his (her) *private sphere* [9, 14].

The granular force \mathbf{f}_g appearing in Eq. (1) represents the sliding friction between contacting people (or between people and walls). Its expression can be seen in Eq. (2). It is assumed to be a linear function of the relative (tangential) velocities $\Delta \mathbf{v}_{ij} \cdot \mathbf{t}_{ij}$ of the contacting individuals. The function $\Theta(r_{ij} - d_{ij})$ returns the argument value if $r_{ij} > d_{ij}$, while κ is a fixed parameter (see Refs. [9–13]).

B. Clustering structures

The time delays during an evacuation process are related to clustering people as explained in Refs. [10, 11]. Groups of contacting pedestrians can be defined as the set of individuals that for any member of the group (say, i) there exists at least another member belonging to the same group (j) for whom $d_{ij} < r_i + r_j$. This kind of structure is called a *human cluster*.

From all human clusters appearing during the evacuation process, those that are simultaneously in contact with the walls on both sides of the exit are the ones that possibly *block* the way out. Thus, we are interested in the minimum number of contacting pedestrians belonging to this *blocking cluster* that are able to link both sides of the exit. We call this minimalistic group as a *blocking structure*. Any blocking structure is supposed to work as a barrier for the pedestrians in behind.

C. The local pressure on the pedestrians

Recall that the social force model (SFM) deals with the pedestrians desire and their private space preservation. Although the desire force \mathbf{f}_d and the social force \mathbf{f}_s are not exactly “physical” quantities (*i.e.* not pair-wise), the movement equation remains valid. Therefore, it can be derived from the virial relation that [15]

$$\left\langle \sum_{i=1}^N \frac{p_i^2}{m_i} + \sum_{i=1}^N \mathbf{r}_i \cdot \mathbf{f}_i \right\rangle = -3\mathcal{P}\mathcal{V} \quad (3)$$

for the set of N pedestrians inside a volume \mathcal{V} . p_i and \mathbf{f}_i are the momentum and total force acting on the individual i (excluding the interaction with the walls). $\langle \cdot \rangle$ corresponds to the mean value along time. The right hand side $-3\mathcal{P}\mathcal{V}$ defines the global pressure on the surface enclosing the volume \mathcal{V} .

The local pressure on a single pedestrian (say, i) corresponds to the forces (per unit area) acting on him due to

the surrounding pedestrians. Following Ref. [15] we can define the “social pressure function” P_i as

$$3P_i V_i = \frac{p_i^2}{m_i} + \frac{1}{2} \sum_{j=1}^{N-1} \mathbf{r}_{ij} \cdot \mathbf{f}_s^{(ij)} \quad (4)$$

where V_i is the volume enclosing the pedestrian i and $\mathbf{r}_{ij} = \mathbf{r}_i - \mathbf{r}_j$. Notice that the inner product $\mathbf{r}_{ij} \cdot \mathbf{f}_s^{(ij)}$ is always positive for repulsive feelings and equals the scalar product $d_{ij} f_s^{(ij)}$.

The second term in Eq. (3) can be split into the sum of the inner products $\mathbf{r}_i \cdot \mathbf{f}_d$ (desire), $\mathbf{r}_i \cdot \mathbf{f}_s$ (social) and $\mathbf{r}_i \cdot \mathbf{f}_g$ (granular). Actually, the sum of the social product depends on the inter-pedestrian distance $d_{ij} f_s^{(ij)}$, while the granular one does not play a role because of orthogonality ($\mathbf{r}_{ij} \cdot \mathbf{f}_g^{(ij)} = 0$). Consequently, the virial relation (3) reads

$$\sum_{i=1}^N \langle 3P_i V_i \rangle = -3\mathcal{P}\mathcal{V} - \sum_{i=1}^N \langle \mathbf{r}_i \cdot \mathbf{f}_d^{(i)} \rangle \quad (5)$$

We should remark that Eq. (5) holds either if the pedestrians are in contact or not. The “social pressure function” P_i makes possible for the individuals to change their behavioural pattern when they come too close to each other or to the walls.

In Appendix A 2 we apply Eq. (5) to a simple example and compare it to our results.

III. NUMERICAL SIMULATIONS

A. Geometry and process simulation

We simulated different evacuation processes for room sizes of 20 m \times 20 m, 30 m \times 30 m and 40 m \times 40 m. The rooms had one or two exit doors on the same wall, as shown in Fig. 1. The doors were placed symmetrically from the mid position of the wall, in order to avoid corner effects. Both doors had also the same width.

At the beginning of the process, the pedestrians were all equally separated in a square arrangement. The occupancy density was set to 0.6 people/m², close to the allowed limiting values in current regulations [16]. They all had random velocities resembling a Gaussian distribution with null mean value. The pedestrians were willing to go to the nearest exit. Thus, all the pedestrians had the desired velocity \mathbf{v}_d pointing to the same exit door if only one door was available, or to the nearest door if two exits were available.

In order to focus on the effects due to dual exits, we only allowed the pedestrians to move individualistically,

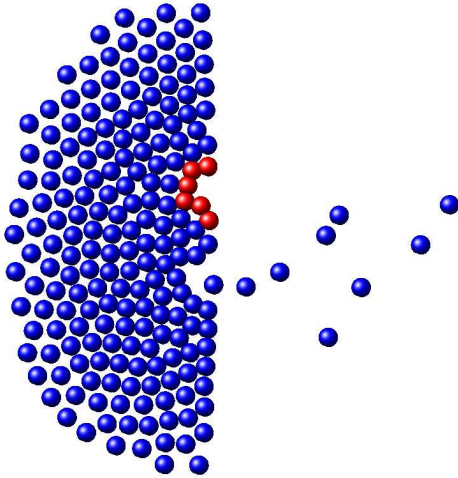


FIG. 1. Snapshot of an evacuation process from a $20\text{ m} \times 20\text{ m}$ room, with two doors. In red we can see a blocking structure around the upper door. The desired velocity was $v_d = 4\text{ m/s}$.

that is, neither leaderships nor herding behaviors were present during the evacuation process. At any time, the pedestrians knew the doors location and tried to escape by their own.

The simulations were supported by LAMMPS molecular dynamics simulator with parallel computing capabilities [17]. The time integration algorithm followed the velocity Verlet scheme with a time step of 10^{-4} s . All the necessary parameters were set to the same values as in previous works (see Refs. [12, 13]). It was assumed that all the individuals had the same radius ($r_i = 0.3\text{ m}$) and weight ($m_i = 70\text{ kg}$). We ran 30 processes for each panic situation, in order to get enough data for mean values computation.

Although the LAMMPS simulator has the most common built-in functions, neither the social force \mathbf{f}_s nor the desire force \mathbf{f}_d were available. We implemented special modules (with parallel computing compatibilities) for the \mathbf{f}_s and \mathbf{f}_d computations. These computations were checked over with previous computations.

The pedestrian's desired direction $\hat{\mathbf{e}}_d$ was updated at each time step. After leaving the room, they continued moving away. No re-entering mechanism was allowed.

B. Measurements conditions

Simulations were run in the same way as in Refs. [12, 13]. Each process started with all the individuals

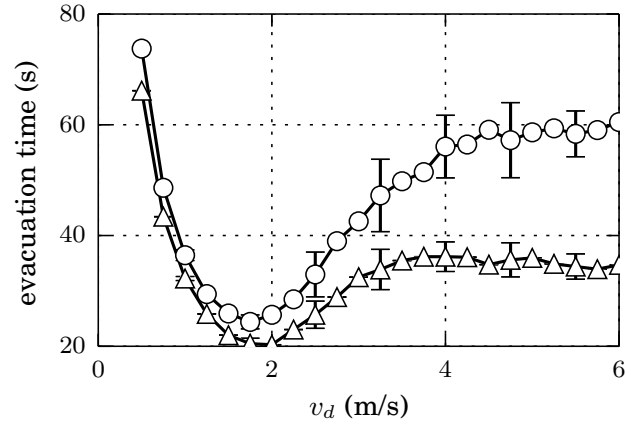


FIG. 2. Mean evacuation time for 160 individuals (seconds) vs. the pedestrian's desired velocity (m/s). Two doors were available for leaving the room (see text for details). Mean values were computed from 30 evacuation processes. Each door was $d_w = 1.2\text{ m}$ width. The desired velocity was $v_d = 4\text{ m/s}$. Two situations are shown: \triangle corresponds to the null separation distance between doors, meaning a single door of $2L$ width. \circ corresponds to the 1 m separation distance between doors.

inside the room. The measurement period lasted until 80% of the occupants left the room. If this condition could not be fulfilled within the first 3000 s, the process was stopped. Data was recorded at time intervals of 0.05τ (cf. Eq. (2a)).

The simulations ran from relaxed situations ($v_d < 2\text{ m/s}$) to very stressing rushes ($v_d = 6\text{ m/s}$). We registered the individuals positions and velocities for each evacuation process. Thus, we were able to compute the “social pressure” through out the process and to trace the pedestrians behavioural pattern.

IV. RESULTS

A. The faster is slower effect

As a starting point, we checked over the “faster is slower” effect for the the room with two doors on the same wall. Fig. 2 shows the recorded evacuation time when the doors are separated a distance of $d_g = 1\text{ m}$ and when no separation exists at all ($d_g = 0$). The latter means a single opening with width equal to two doors. Both cases (with or without separation) exhibit a change in their corresponding derivatives. Thus, the “faster is slower” effect is achieved following the same qualitative response as the one found in previous works for rooms with a single exit [9, 10].

The evacuation time for separated doors in Fig. 2 is always above the time required to evacuate the pedestrians through the single opening (*i.e.* null separation).

For $v_d = 6$ m/s, the single opening improves the evacuation performance in half of the time that demands the $d_g = 1$ m separation configuration. Other separation distances (not shown) exhibit the same qualitative pattern as the example presented in Fig. 2. Therefore, it is clear that while the total width of the opening remains unchanged, splitting this width into two symmetric exits may affect significantly the evacuation performance.

The results shown in Fig. 2 are in agreement with the conclusions reported in Ref. [6]. Any door separation distance less than $4d_w$ (see caption in Fig. 2) produce a “slow-down” in the evacuation performance. However, we did not come to consensus on the reasons of this slow-down, as expressed in Ref. [6]. After running some animations, we realized that the “disruptive interference effect” mentioned there could not be the main reason for the increase in the evacuation delays.

We made further inquiries on the $d_g = 0$ and $d_g > 0$ scenarios. The former is investigated in Section IV B, while the latter is left to Section IV C.

B. The single door vs. the null separation

Recall that the $d_g = 0$ scenario corresponds to one door with an opening equal to twice its width (see Section IV A). According to Ref. [8], this widening is expected to affect the evacuation performance.

1. The stop-and-go process

Fig. 3 illustrates on how the evacuation performance can be improved as the opening becomes wider. Fig. 3a corresponds to the single door, while Fig. 3b corresponds to the null separation situation (wider opening). We can see the (normalized) pressure and velocity evolution of a tagged pedestrian that rushes from $(x, y) = (12.35 \text{ m}, 8.45 \text{ m})$ to the exit. His (her) evacuation time is reduced by five when the opening widens by three (see Fig. 3). This is in partial agreement with Ref. [7] since the widening improves the flux of evacuating people, but we cannot assure that the flux per unit width decreases, as the authors in Ref. [7] suggest.

The tagged pedestrian in Fig. 3 increases his (her) velocity towards an asymptotic value at the beginning of the processes. This value corresponds to the desired velocity $v_d = 4$ m/s. But close to $t = 2$ s, the pedestrian suddenly stops because of the clogging around the exit. Clogging is also responsible for the pressure increase, as shown in both Fig. 3a and Fig. 3b (for details on how the pressure was computed, see below in this section). Notice, however, that any further fluctuation of the pressure acting on the tagged pedestrian corresponds to an inverse fluctuation on the velocity. Thus, the pedestrian

is able to reach the exit following a stop-and-go process.

The instantaneous pressure acting on a single pedestrian can be computed from Eq. 4. If we neglect the momentum p_i for any slow moving pedestrian, then $3P_i V_i$ in Eq. 4 equals the sum of the products $d_{ij} f_s^{(ij)}$. Actually, not all the inter-pedestrian distances d_{ij} need to be computed since only the first neighbors contribution to the social force become relevant. The magnitude $3P_i V_i$ is the one represented in Fig. 3a and Fig. 3b (normalized by $3P_{\max} V_i$).

The maximum pressure values $3P_{\max} V_i$ in Fig. 3a and Fig. 3b are 8783 N.m and 7103 N.m, respectively. The corresponding mean pressure values (after the first 2 s) are 80% and 55% of the respective maximum values. This means that although the reported maximum pressure is quite similar in both situations, there is a noticeable bias in the mean values. The wider opening seems to release pressure from time to time. Consequently, the stop-and-go processes are somehow different for the single door with respect to the $d_g = 0$ situation (the wider opening).

2. The pressure and stream patterns

For a better understanding on how the pedestrians are (intermittently) released from high pressures in the wide opening situation, we pictured the whole scene into a pressure contour map and a mean stream path map for all the individuals. Fig. 4a shows the pressure levels ($3P_i V_i$) for the clogging area. The warm colors are associated to high pressure values. These values are close to the corresponding maximum pressure values (not shown). Thus, the warm regions define the places where the pedestrians slow down most of the time. They are expected to get released only for short periods of time. On the contrary, the regions represented in cold colors (low mean pressure) are those where the individuals are supposed to get released for longer time periods.

Fig. 4b represents the mean stream lines during the evacuation process. It completes the stop-and-go picture since it exhibits the released paths for leaving the room. Notice that the stream lines pass through the low pressure regions. That is, it can be seen in Fig. 4b that the stream lines gather along the middle of the clogging area, where “cold” pressure colors can be found (cf. Fig. 4a). The “warm” pressure colors are placed on the sides of this region.

We checked over the trajectory of the tagged pedestrian represented in Fig. 3b and we observed that he (she) managed to get out of the room through the path where the stream lines gather. Thus, Fig. 3b resembles the stop-and-go process for the pedestrians passing through the middle of the clogging area, that is, along the low pressure (middle) region. The pedestrians on the sides

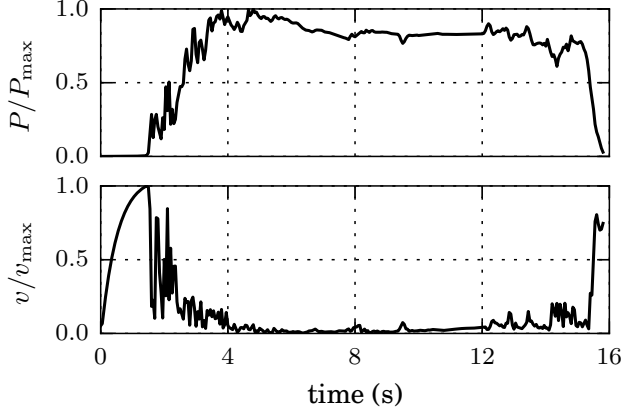
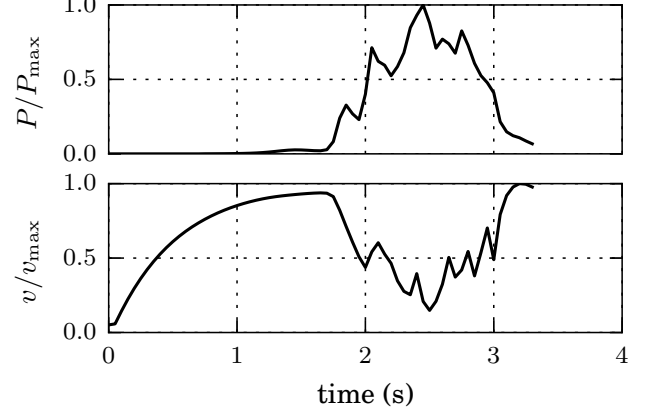
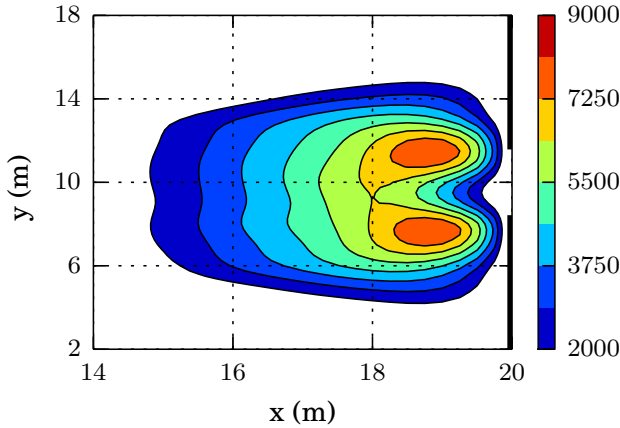
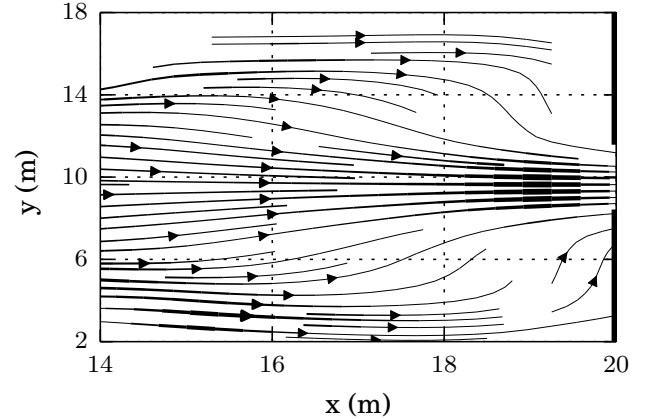
(a) Opening of $d_w = 1.2$ m width (single door exit).(b) Opening of $3d_w = 3.6$ m width (null separation).

FIG. 3. Normalized pressure and velocity on a single pedestrian during an evacuation process. Data was recorded from the initial position at $x = 12.35$ m and $y = 8.45$ m, until the individual left the room ($x > 20$ m). The pedestrians desired velocity was $v_d = 4$ m/s. Two situations are shown: (a) evacuation through a single door of width $d_w = 1.2$ m. (b) evacuation through an opening of $3d_w = 3.6$ m (resembling the null separation situation for two doors of width $1.5L$).



(a) Mean pressure contour lines. The scale bar on the right is expressed in N.m units (see text for details). Level colors can be seen in the on-line version only.



(b) Mean stream lines. The lines connect the normalized velocity field (v/v_{\max}). The arrows indicate the stream direction.

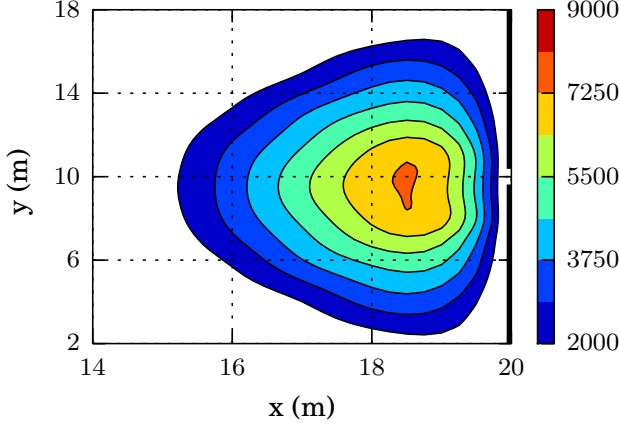
FIG. 4. Mean pressure and stream lines computed from 30 evacuation processes until 100 pedestrians left the room ($20\text{ m} \times 20\text{ m}$ size). Data was recorded on a square grid of $1\text{ m} \times 1\text{ m}$ and then splined to get smooth curves. The thick black lines at $x = 20$ m represent the walls on the right of the room. There is only one opening of $3d_w = 3.6$ m width (null separation distance between doors of width $3L/2$). The pedestrian's desired velocity was $v_d = 4$ m/s.

of this region (high pressure region) are expected to slow down since Fig. 4b shows no stream lines to the exit.

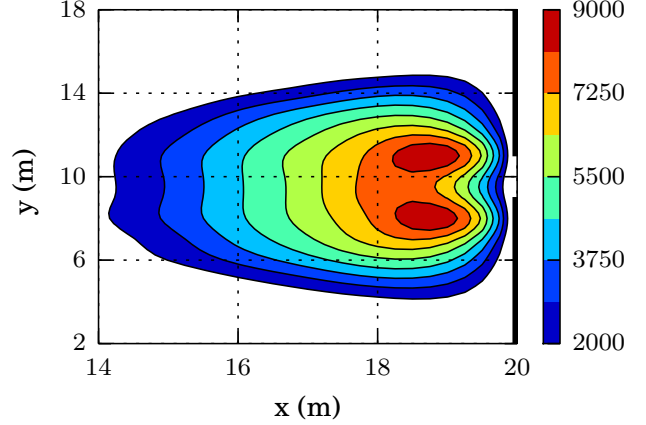
Recalling the results in Fig. 3a for the same tagged individual as in Fig. 3b, we realize that the single door scene is likely to differ from the $d_g = 0$ situation since both patterns (for the same individual) do. Thus, we examined the pressure contour map for the single door and for an opening of twice the single door width. The results are shown in Fig. 5. Fig. 5b exhibits a similar pressure map pattern as Fig. 4a, but the single door pressure map

in Fig. 5a does not. For the single door situation, we do not observe the lower pressure pathway in the middle of the clogging area. Instead, high pressure is acting on the pedestrians, as shown in the (normalized) pressure evolution in Fig. 3a. The corresponding velocity evolution (Fig. 3a) informs that the pedestrians in this region experience a slow down.

At this stage of the investigation we are able to point out a few conclusions. The widening of the single door increases the pedestrian's flux, as asserted in Ref. [7]. In



(a) Opening of $d_w = 1.2$ m width (single door exit).



(b) Opening of $2d_w = 2.4$ m width (null separation distance between doors of width L).

FIG. 5. Mean pressure contour lines computed from 30 evacuation processes until 100 pedestrians left the room ($20\text{ m} \times 20\text{ m}$ size). The scale bar on the right is expressed in N.m units (see text for details). The thick black lines at $x = 20$ m represent the walls on the right of the room. The pedestrian's desired velocity was $v_d = 4\text{ m/s}$. The contour lines were computed on a square grid of $1\text{ m} \times 1\text{ m}$ and then splined to get smooth curves. Level colors can be seen in the on-line version only.

the single door situation, the pedestrians experience a slow down close to the exit. These time delays have been associated to blocking structures (see Refs. [10, 11]) and causes the pressure acting on the nearby individuals to rise. Fig. 5a resembles this situation. However, as the opening widens (*i.e.* the null separation situation), the pressure pattern changes qualitatively (see Fig. 4a and Fig. 5b), allowing the pedestrians in the middle of the clogging area to make a pathway to the exit. This pathway corresponds to the breaking of the blocking structures.

C. Separated doors

The second relevant distance mentioned in Ref. [8] is the doors separation distance. We will fix the door width $d_w = 1.2\text{ m}$ and focus only on the evacuation processes from a room with two doors symmetrically placed on the same side of the room.

It has been shown in Fig. 2 that separating the doors a distance $d_g = 1\text{ m}$ worsens the evacuation performance. We further explored this worsening by increasing d_g at steps of 0.5 m , starting from the null separation distance. Fig. 6 shows the mean evacuation time and the corresponding error bars (indicating the $\pm\sigma$ limits). The desired velocity was set to $v_d = 4\text{ m/s}$, achieving the “faster is slower” scenario.

The evacuation time as a function of d_g shown in Fig. 6 is one of our main results. The worsening in the evacuation performance rises to a maximum value, and surprisingly, its derivative changes sign for $d_g > 1\text{ m}$. Thus,

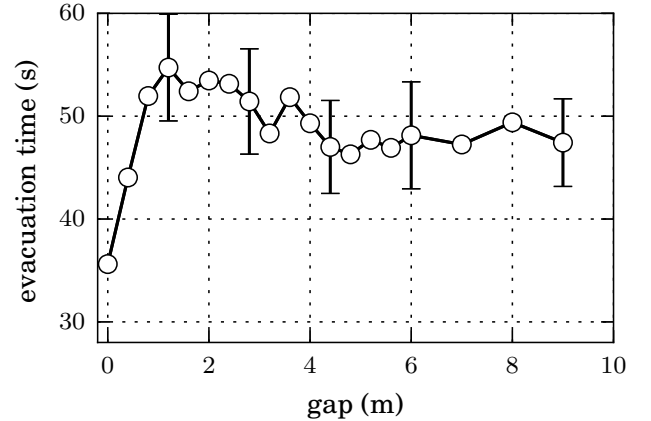


FIG. 6. Mean evacuation time for 225 pedestrians (room of $20 \times 20\text{ m}$ size) as a function of the doors separation distance. Mean values were computed from 30 evacuation processes until 160 pedestrians left the room. Each door was $d_w = 1.2\text{ m}$ width for non-vanishing gaps. The null gap means a single door of $2L$ width. The desired velocity was $v_d = 4\text{ m/s}$.

$d_g = 1\text{ m}$ appears to be the worst evacuation scenario for the $20\text{ m} \times 20\text{ m}$ room with 225 individuals and two doors of $d_w = 1.2\text{ m}$ each (see Fig. 6).

Notice that Fig. 6 is not in complete agreement with the literature [6, 8]. As outlined in Section I, it has been argued that the optimal separation distance (gap) d_g should be bounded between $4d_w$ and $L - 4d_w$ (L means the room side, while d_w is the doors width). An inspection of Fig. 6 confirms this, although very small values of d_g can also enhance the evacuation time. Thus, it is not

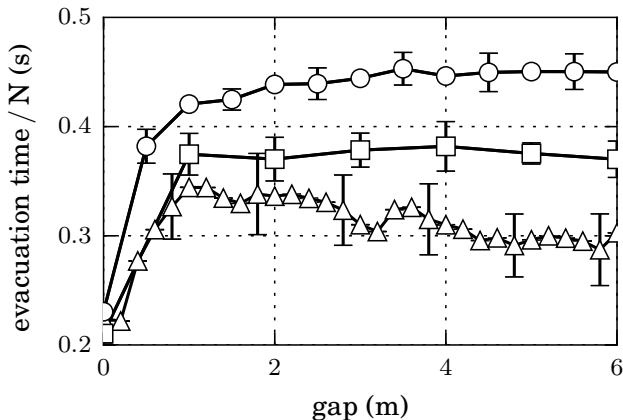


FIG. 7. Mean evacuation time per total number of pedestrians that left the room (N), as a function of the doors separation distance. Mean values were computed from 30 evacuation processes. Each door was $d_w = 1.2$ m width for non-vanishing gaps. The null gap means a single door of $2L$ width. Three situations are shown: \triangle corresponds to the 20×20 m room when 160 pedestrians left the room, \square corresponds to 30×30 m room when 530 pedestrians left the room, and \circ corresponds to 40×40 m room when 865 pedestrians left the room. The desired velocity was $v_d = 4$ m/s.

completely true that the “disruptive interference effect” causes a slow down if $d_g < 4d_w$.

The critical distance $4d_w$ has also been identified in the literature as the separation distance necessary to distinguish two independent pedestrian bulks around each door [6]. We checked over this assertion by computing the mean evacuation time for an increasing number of pedestrians (and room sizes). We kept the pedestrian density unchanged (at $t = 0$) for all the simulation processes. Fig. 7 exhibits the mean evacuation time per pedestrian as a function of the separation distance (*i.e.* gap). We divided the evacuation time by the total number of pedestrians for visualization reasons.

The results shown in Fig. 7 were not expected. The evacuation time settles to an asymptotic value for separation distances $d_g > 5$ m. This means that the critical distance $4d_w$ and the bulk separation distance are actually not related, as proposed in Ref. [6]. The mean evacuation time becomes almost independent of the separation distances d_g despite that the clogging areas around the doors might still overlap.

Fig. 7 also shows that the derivative not always changes sign at $d_g \simeq 1$ m. Furthermore, as the number of pedestrians is increased for $d_g > 1$ m, the evacuation time derivative raises to positive values. The greater the number of pedestrians, the worst evacuation time (per individual). This appears to occur for $d_g > 1$ m, regardless of the crowd size. That is, according to Fig. 7, there exists a separation distance value $d_g \simeq 1$ m where the evacuation derivative changes sharply to negative or positive values

(for $d_g > 1$ m). This phenomenon has not been studied in the literature, to our knowledge.

We can resume the results in Fig. 7 in the following way: the evacuation time rises when the doors separation increases from a wide opening (null separation distance) to the distance $d_g \simeq 1$ m. At this gap, the evacuation time derivative changes sharply, entering a much slowly varying regime towards an asymptotic value (for $d_g \gg 1$ m). The former can be identified as a regime for small values of d_g , while the latter is valid for moderate to large values of d_g . The fact that a sharp change occurs at $d_g \simeq 1$ m, no matter the crowd size, suggests that both regimes are somehow different in nature. This moved us to explore the two regimes separately.

1. The regime for $d_g < 1$ m

Our starting point is the pressure contour map, since we can easily compare the current patterns with those presented in Section IV B 2. Fig. 8a shows the mean pressure pattern for the separation distance $d_g = 1.5$ m, that is, close to the gap value where the sharp change in the derivative occurs. The differences between Fig. 8a and Fig. fig:2and4 are noticeable. We can now see a wide region in the center of the clogging area representing the high pressure ($3P_i V_i$) acting on each pedestrian (warm color in Fig. 8a). The regularity in the color of this region is meaningful: the high pressure acting on the pedestrians does not allow a regular stream (pathway) to the exit. This is in agreement with the evacuation time worsening shown in Fig. 6.

Fig. 8a suggests that blocking structures might be present for long time periods, since the pedestrians cannot manage to get out easily. We examined this possibility through the *blocking probability*. In this context, the blocking probability is associated to the ratio between the time that each door remains blocked with respect to the total evacuation time (cf. Section II B). Fig. 9 presents two kinds of blockings: the simultaneous blocking of both doors, and the blocking of a single door (say, the one on the left). The former connects the left most wall with the right most wall, but does not contact the separation wall in the middle of the walls. The latter connects the walls on both sides of the selected door (say, the one on the left).

According to Fig. 9, the single door blockings are not relevant until $d_g \simeq 1$ m, while the simultaneous blockings weaken as the gap (separation distance d_g) increases. The single door blockings resemble the response in Fig. 6, and thus, we conclude that this kind of blockings should play an important role in the increase of the evacuation time for small gaps d_g . Notice that single door blocking probability explains the 75% of the evacuation time, as can be seen in Fig. 9.

The results so far moved us to focus closer on the dy-

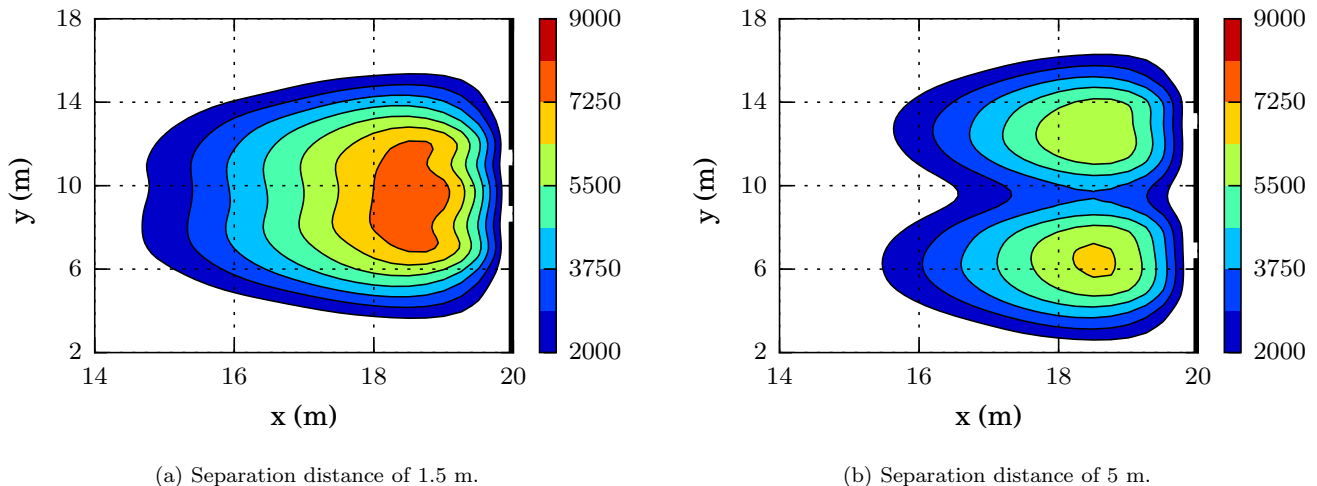


FIG. 8. Mean pressure contour lines computed from 30 evacuation processes until 100 pedestrians left the room ($20\text{ m} \times 20\text{ m}$ size). The scale bar on the right is expressed in N.m units (see text for details). The thick black lines at $x = 20\text{ m}$ represent the walls on the right of the room. The pedestrian's desired velocity was $v_d = 4\text{ m/s}$. The contour lines were computed on a square grid of $1\text{ m} \times 1\text{ m}$ and then splined to get smooth curves. Level colors can be seen in the on-line version only.

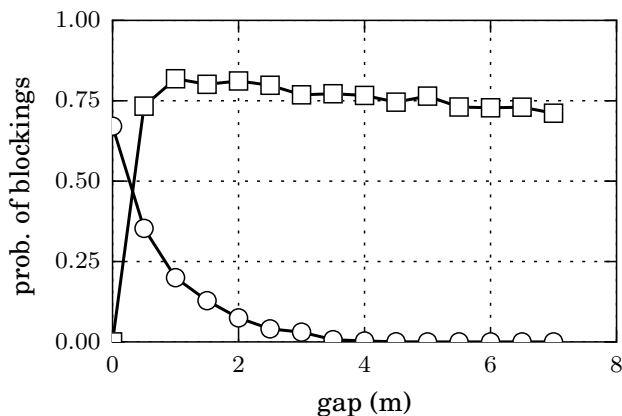


FIG. 9. Ratio between time steps including blocking structures and the total number of time steps for 30 evacuation processes, as a function of the doors separation distance. The room size was $20 \times 20\text{ m}$ with 225 occupants. Each door was $d_w = 1.2\text{ m}$ width for non-vanishing gaps. The null gap means a single door of $2d_w$ width. The desired velocity was $v_d = 4\text{ m/s}$. ○ corresponds blocking structures connecting both the left side wall of the left door with the right side wall of the right door (see text for details). □ corresponds to blocking structures connecting both sides of a single door (see text for details).

namics around each door. We watched many animations of the evacuation process for gap distances between the null separation to $d_g = 1.5\text{ m}$ (not shown). We realized that single door blockings hold if the gap is large enough to stop at least two pedestrians. That is, any blocking structure enclosing a single door can hold for some time if the pedestrians at the end of the structure (and in con-

tact with the walls) do hardly leave the structure. Two pedestrians are needed at the gap wall to ensure that both doors remain blocked.

We want to call the attention on the fact that in the $d_g \simeq 1\text{ m}$ scenario, the kind of simultaneous blocking without contacting the gap wall, is replaced by the kind of single door blockings acting (usually) simultaneously. This achieves a qualitative different pressure and stream pattern. As shown in Fig. 5b, the widening of the exit allows a pathway through the middle of the clogging area. This is likely to occur even for very small gaps (see Fig. 9). However, the single door blockings follow a pressure pattern similar to Fig. 5a on each door. What we see in Fig. 8a is the combined pattern built from two single door patterns as in Fig. 5a.

We conclude from the analysis of small gaps ($d_g < 1\text{ m}$) that a door separation distance roughly equal to two pedestrian widths is critical. This distance allows persistent single door blockings. Small distances (close to the null separation) do not actually allow single door blockings to hold for long time. Thus, the role of $d_g = 2d_w$ is decisive to move the evacuation process from one regime to another.

2. The regime for $d_g > 1\text{ m}$

Fig. 9 shows that the single door blockings (see Section IV C 1) remains around 75% of the total evacuation time for $d_g > 1\text{ m}$ (225 individuals in the room). We also computed this magnitude for situations with increasing number of individuals (see Fig. 10). The probability of single door blockings approaches unity as the crowd

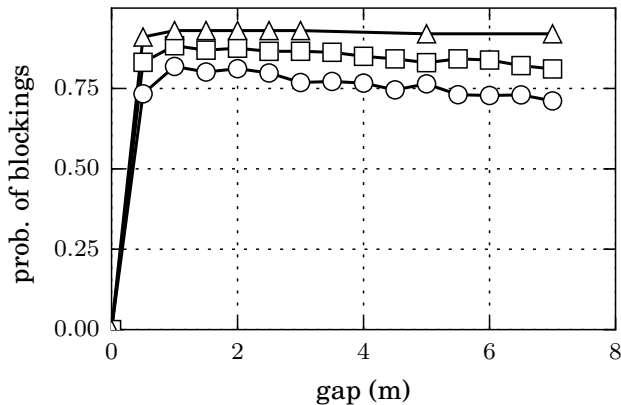


FIG. 10. Ratio between time steps including blocking structures and the total number of time steps for 30 evacuation processes, as a function of the doors separation distance. The only blocking structures considered were those connecting both sides of one single door (see text for details). Each door was $d_w = 1.2$ m width for non-vanishing gaps. The null gap means a single door of $2d_w$ width. Three scenarios are shown: ○ corresponds to the room of size 20×20 m with 225 occupants and a desired velocity of $v_d = 4$ m/s. □ corresponds to the room of size 20×20 m with 225 occupants and a desired velocity of $v_d = 6$ m/s. △ corresponds to the room of size 40×40 m with 961 occupants and a desired velocity of $v_d = 4$ m/s.

size increases. This means, according to our definition of blocking probability, that the blocking time raises as the number of individuals increases. The gap distance, however, does not play a role for $d_g > 1$ m.

There is a noticeable difference between the evacuation time shown in Fig. 7 and the blocking probability exhibited in Fig. 10. The derivative changes sign in the former (for increasing number of pedestrians), but it does not in the latter. Therefore, the blocking time cannot be considered as the reason for this changes.

We examined many animations of the evacuation process for an increasing number of pedestrians and separation distances. We also checked the pressure patterns for $d_g > 4d_w$ (see Fig. 8b as an example). We came to the conclusion that since the evacuation derivative in Fig. 7 changes with an increasing number of individuals, the whole bulk should be involved in this phenomenon. Therefore, we focused our investigation on the pressure contribution of the whole bulk.

Eq. 5 relates the “social pressure function” (left-hand side) with the desire force contribution (right-hand side). That is, an increase in the desire force of the individuals (*i.e.* anxiety levels) means an increase in the bulk “social pressure”. A simple example on the Eq. 5 computation can be found in the Appendix below.

Fig. 11 shows the evacuation time as a function of the separation distance for two different desired velocities.

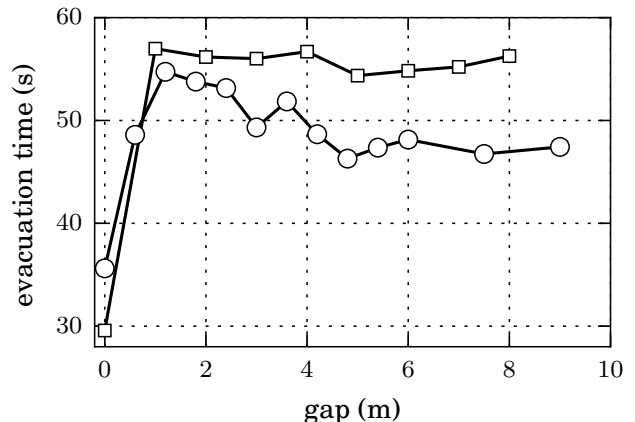


FIG. 11. Mean evacuation time for 225 pedestrians (room of 20×20 m size) as a function of the doors separation distance. Mean values were computed from 30 evacuation processes until 160 pedestrians left the room. Each door was $d_w = 1.2$ m width for non-vanishing gaps. The null gap means a single door of $2L$ width. ○ corresponds to pedestrians with desired velocity of $v_d = 4$ m/s. □ corresponds to pedestrians with desired velocity of $v_d = 8$ m/s.

As expected, the sharp change in the derivative occur around $d_g = 2d_w$. Also the derivative changes as the desired velocity is increased (*i.e.* higher anxiety level). This confirms that the social pressure is responsible the derivative behaviour shown in Fig. 7.

We conclude from the analysis of large gaps ($d_g > 1$ m) that the evacuation time is controlled by the social pressure in the bulk. The crowd size and the desired velocity v_d affects the pressure acting on the pedestrians. But no further changes in the evacuation time can be noticed for $d_g > 4d_w$. This means that the asymptotic evacuation value does not depend strongly on whether the bulks around each door are completely independent.

V. CONCLUSIONS

We examined in detail the evacuation of pedestrians for the situation where two contiguous doors are available for leaving the room. Throughout Section IV we presented results on the evacuation performance under high anxiety levels and increasing number of pedestrians. Both conditions exhibit the novel result that a worsening in the evacuation time as the door separation distance d_g increases from the null value to roughly the width of two pedestrians. Special situations may enhance the evacuation performance for larger values of d_g .

Two regimes were identified as the d_g values increased from $d_g = 0$ to $d_g > d_w$ (2 pedestrians width). The range $0 \leq d_g \leq 2d_w$ worsened the evacuation performance for all the explored situations, while the range $d_g > 2d_w$ did enhance the evacuation time for relatively small crowds

and moderate anxiety levels. We realized that the sharp change in the evacuation behaviour at $d_g = 2d_w$ corresponded to qualitative differences in the pedestrian dynamics close to the exits.

After a detailed comparison of the dynamics for the single door situation and for two doors very close to each other (that is $d_g < 2d_w$), we concluded that the blocking structures (*i.e.* blocking archs) around the openings were released intermittently, allowing the pedestrians to leave the room in a stop-and-go process. But, as the separation distance approached $2d_w$, the blocking archs were restored around each door, resembling the blocking situation of two a single doors. This changes only affected the local dynamics (close to the doors), while the crowd remained gathered into a single clogging area.

Starting at $d_g = 2d_w$ allows the single door blocking structures to become relevant even for large values of d_g (see Fig.9). No further qualitative changes were observed locally around each door. However, increasing the crowd size (N) or the pedestrian's anxiety level (v_d) slowed down the evacuation. Both magnitudes are linked to the pressure acting on the pedestrians, and therefore, enhanced the “faster is slower” affects.

For a better understanding of the relationship between N , v_d and the pressure in the bulk, a simple lane example complemented our analysis. It was shown that the classical virial expression is still suitable for the investigation of social systems.

ACKNOWLEDGMENTS

C.O. Dorso is a main researcher of the National Scientific and Technical Research Council (spanish: Consejo Nacional de Investigaciones Científicas y Técnicas - CONICET), Argentina. G.A. Frank is an assistant researcher of the CONICET, Argentina. I.M. Sticco has degree in Physics.

Appendix A: The lane example

We decided to open this supplementary section in order to make clear the meaning of the “social pressure” acting on an individual and the collective pressure (that is, the *bulk* pressure) on a set of individuals. We will follow a simple example as a guide for more general situations.

1. The social pressure

Fig. 12 represents a lane of individuals pushing to the right. The ending wall prevents the individuals from moving. All the pedestrians in the lane are at their equilibrium positions $x_1, x_2, \dots, x_i, \dots, x_N$, while the wall is placed at the position $x_0 = 0$ (see Fig. 12).

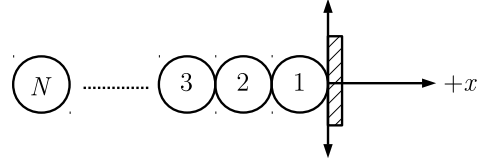


FIG. 12. Lane of individuals pushing to the right. The horizontal axis indicates the positive direction.

The pedestrians push to the right acknowledging a desired force $f_d^{(i)} = mv_d/\tau$, according to Eq. (2). The social repulsion feelings balance this desire force, but only the contacting neighbors are relevant to these feelings. Thus, the balance equation for any pedestrian in the lane reads

$$f_s^{(i,i+1)} - f_s^{(i,i-1)} + \frac{mv_d}{\tau} = 0 \quad (\text{A1})$$

for $f_s^{(i,j)}$ meaning the repulsive feelings of pedestrian i due to the presence of pedestrian j . Notice that the boundary condition at the wall-end is $x_0 = 0$ (Dirichlet condition), while the condition at the free end is $f_s^{(N,N+1)} = 0$ (Neumann condition). The forces on the pedestrians can be obtained recursively from Eq. A1, starting at the free ended individual ($i = N$). The resulting expression is

$$f_s^{(i,i-1)} = (N - i + 1) \frac{mv_d}{\tau}, \quad i = 1, \dots, N \quad (\text{A2})$$

while the corresponding positions $x_1, x_2, \dots, x_i, \dots, x_N$ are obtained by a backward substitution of the social forces expressed in Eq. 2, starting at the wall-end

$$x_i = x_{i-1} - (r_i + r_{i-1}) + B \ln \left[(N - i + 1) \frac{mv_d}{A\tau} \right] \quad (\text{A3})$$

Our intuition suggests that the pressure on a single pedestrian P_i corresponds to the forces acting on him (her) (per unit area) due to the neighboring pedestrians. We can further assert this from the “social pressure function” definition (4)

$$P_i = \frac{1}{2} \left[\frac{x_i - x_{i+1}}{3V_i} f_s^{(i,i+1)} + \frac{x_{i-1} - x_i}{3V_i} f_s^{(i,i-1)} \right] \quad (\text{A4})$$

where the magnitude $x_{ij}/3V_i$ corresponds to the (inverse) effective surface of the pedestrian. For individuals modeled as hard spheres, the inter-pedestrian distance is $x_{ij} = 2r_i$ and the volume is $V_i = 4\pi r_i^3/3$. Thus,

$$P_i = \frac{1}{4\pi r_i^2} \left[f_s^{(i,i+1)} + f_s^{(i,i-1)} \right] \quad (\text{A5})$$

as expected for the individual pressure.

2. The bulk pressure

We can first check over the virial relation (5) through the expression (A4). Adding the terms for the lane of N pedestrians and replacing the first and last term with the corresponding boundary condition, gives

$$\left\{ \begin{array}{l} 3P_1V_1 = \frac{x_1}{2} f_s^{(1,2)} - \frac{x_2}{2} f_s^{(1,2)} \\ 3P_2V_2 = \frac{x_2}{2} [f_s^{(2,3)} - f_s^{(2,1)}] - \frac{x_3}{2} f_s^{(2,3)} + \frac{x_1}{2} f_s^{(2,1)} \\ 3P_3V_3 = \frac{x_3}{2} [f_s^{(3,4)} - f_s^{(3,2)}] - \frac{x_4}{2} f_s^{(3,4)} + \frac{x_2}{2} f_s^{(3,2)} \\ \dots \\ 3P_NV_N = -\frac{x_N}{2} f_s^{(N,N-1)} + \frac{x_{N-1}}{2} f_s^{(N,N-1)} \end{array} \right. \quad (\text{A6})$$

These are the local pressures on each pedestrian due to the contacting neighbors (and excluding the wall). Adding the terms results in the virial relation, as expressed in (5)

$$\begin{aligned} \sum_{i=1}^N 3P_iV_i &= (x_1 - x_2)f_s^{(1,2)} + (x_2 - x_3)f_s^{(2,3)} + \dots \\ &\quad + (x_{N-1} - x_N)f_s^{(N,N-1)} \\ &= x_1 \frac{Nmv_d}{\tau} - \sum_{i=1}^N x_i \frac{mv_d}{\tau} \end{aligned} \quad (\text{A7})$$

where the first term on the right corresponds to the global pressure $-3\mathcal{PV}$. Notice that x_1 is negative, and thus, $3\mathcal{PV}$ is defined as a positive magnitude. The last term is also positive, adding pressure to the bulk due to the desire forces.

The virial relation (5) allows to compute the *bulk* pres-

sure on a group of pedestrians. For example, the pressure on the M pedestrians closest to the wall corresponds to the force acting on this group due to the other $N - M$ pedestrians. According to Eq. (5), the pressure on the M individuals is

$$\sum_{i=1}^M 3P_iV_i = -3\mathcal{PV} - \sum_{i=M+1}^N 3P_iV_i - \sum_{i=1}^N x_i \frac{mv_d}{\tau} \quad (\text{A8})$$

The *bulk* pressure on the first M individuals increases as more individuals are included in the crowd. This can be verified by evaluating Eq. (A7) and Eq. (A8) for increasing values of N .

The Eqs. (A2) and (A3) allow to compute the pedestrian pressure profile as a function of the distance to the wall. The profile is qualitatively similar to the one measured during an evacuation process. Fig. 13 represents the histogram for the pressure on each pedestrian.

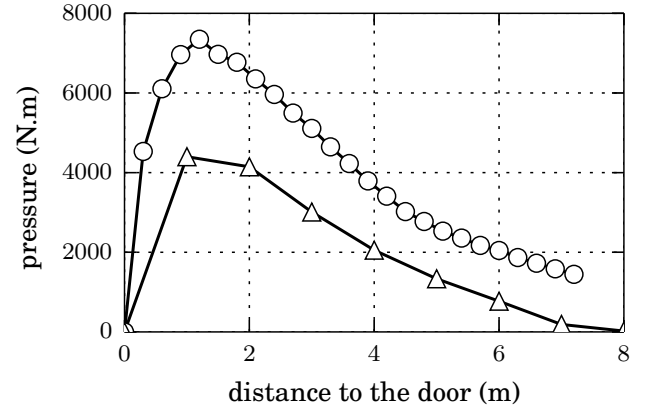


FIG. 13. Mean pressure as a function of the distance to the exit. The room was 20 m \times 20 m size and included one door of $d_w = 1.2$ m width. Mean values were computed from 30 evacuation processes, until 100 pedestrians left the room. The desired velocity was $v_d = 4$ m/s. The distance to the door was binned into equal intervals of 0.3 m or 1 m. The \circ symbols correspond to bins of 0.3 m long. The symbols \triangle correspond to bins of 1 m long, but the recording was restricted to $9.5 \text{ m} \leq y \leq 10.5 \text{ m}$ (see text for details).

[1] W. Cheng, S. Lo, Z. Fang, and C. Cheng, Structural Survey **22**, 201209 (2004).
 [2] OSHA, Occupational Safety & Health Administration Standards 29-CFR **1910.36(b)**, 1 (2015).
 [3] FBC2010, Florida Building Code Handbook **1015.1**, 90 (2010).
 [4] FBC2010, Florida Building Code Handbook **1008.1**, 81 (2010).
 [5] A. Kirchner and A. Schadschneider, Physica A **312**, 260

(2002).
 [6] G. Perez, G. Tapang, M. Lim, and C. Saloma, Physica A **312**, 609 (2002).
 [7] Z. Daoliang, Y. Lizhong, and L. Jian, Physica A **363**, 501 (2006).
 [8] T. Huan-Huan, D. Li-Yun, and X. Yu, Physica A **420**, 164 (2015).
 [9] D. Helbing, I. Farkas, and T. Vicsek, Nature **407**, 487 (2000).

- [10] D. Parisi and C. Dorso, *Physica A* **354**, 606 (2005).
- [11] D. Parisi and C. Dorso, *Physica A* **385**, 343 (2007).
- [12] G. Frank and C. Dorso, *Physica A* **390**, 2135 (2011).
- [13] G. Frank and C. Dorso, *International Journal of Modern Physics C* **26**, 1 (2015).
- [14] D. Helbing and P. Molnár, *Physical Review E* **51**, 4282 (1995).
- [15] T. W. Lion and R. J. Allen, *Journal of Physics: Condensed Matter* **24**, 284133 (2012).
- [16] M. Mysen, S. Berntsen, P. Nafstad, and P. G. Schild, *Energy and Buildings* **37**, 1234 (2005).
- [17] S. Plimpton, *Journal of Computational Physics* **117**, 1 (1995).